

Novel non-magnetic hard boride Co_5B_{16} synthesized under high pressure

Elena Bykova,^{1,2, a)} Alexander A. Tsirlin,³ Huiyang Gou,^{1,2} Leonid Dubrovinsky,¹
Natalia Dubrovinskaia²

¹*Bayerisches Geoinstitut, Universität Bayreuth, D-95440 Bayreuth, Germany*

²*Material Physics and Technology at Extreme Conditions, Laboratory of Crystallography, University of Bayreuth, D-95440 Bayreuth, Germany*

³*National Institute of Chemical Physics and Biophysics, Akadeemia tee 23, EE-12618 Tallinn, Estonia*

^{a)}Electronic mail: Elena.Bykova@uni-bayreuth.de

A first cobalt boride with the Co:B ratio below 1:1, Co_5B_{16} , was synthesized under high-pressure high-temperature conditions. It has a unique orthorhombic structure (space group $Pmma$, $a = 19.1736(12)$, $b = 2.9329(1)$, and $c = 5.4886(2)$ Å, R_1 (all data) = 0.037). The material is hard, paramagnetic, with a weak temperature dependence of magnetic susceptibility.

1. Introduction

Transition-metal (TM) borides are interesting in both fundamental and applied aspects. Their high hardness related to the rigid boron network can be superimposed on interesting magnetic and electronic properties driven by the transition-metal ion. For example, FeB_4 is a non-magnetic iron boride that becomes superconducting below 2.9 K.^{1,2} It is a unique material that combines superhardness and superconductivity.² However, it is metastable and can be prepared under high pressure only. In contrast, Fe-rich borides, such as Fe_2B and FeB , can be synthesized at ambient pressure. They are ferromagnets with remarkably high Curie temperatures (T_C) of 1015 K and 593 K, respectively.³ On general grounds, one expects that the decrease in the Metal:B ratio will suppress the magnetism,⁴ while keeping the system metallic and giving rise to interesting low-temperature effects, such as superconductivity. Therefore, B-rich transition-metal borides remain tantalizing, but also difficult to synthesize.

Cobalt borides share many similarities with the Fe-B compounds. Co_2B and CoB are isostructural to Fe_2B and FeB , respectively, but they show a somewhat weaker magnetism. Co_2B becomes ferromagnetic below $T_C = 433$ K, whereas CoB is a paramagnetic metal.³ Remarkably, no cobalt borides with the Co:B ratio below 1:1 have been reported. Here, we present synthesis, crystal structure, magnetic properties, and electronic structure of a novel hard boride Co_5B_{16} that fills this gap. This new compound reveals paramagnetic behavior related to a nearly complete occupation of the localized Co 3d states.

2. Material and methods

2.1. Starting materials and synthesis

Single-crystals of Co_5B_{16} were synthesized at pressure of 15 GPa and a temperature of 1873 - 1573 K (heating duration was 40 min) in the Kawai-type multi-anvil apparatus⁵ using a 1000-ton (Hymag) hydraulic press. As starting materials we used a cobalt wire (Goodfellow, 99.5% purity) and a boron powder (Chempur Inc., 99.99% purity) which were enclosed into a *h*-BN capsule. The pressure was calibrated based on the phase transitions of standard materials and the temperature was determined using a W3Re/W25Re thermocouple.

2.2. Single crystal XRD

A black lustrous prismatic crystal of Co_5B_{16} with a size of $0.07 \times 0.05 \times 0.05$ mm³ was used for the crystal structure investigation by means of single-crystal X-ray diffraction. The diffraction data were collected at ambient temperature using a four-circle Oxford Diffraction Xcalibur diffractometer ($\lambda = 0.7107$ Å) equipped with an Xcalibur Sapphire2 CCD detector. The intensities of the reflections were measured by step scans in omega-scanning with a narrow step width of 0.5° . The data collection and their further integration were performed with the CrysAlisPro software.⁶ Absorption corrections were applied empirically by the Scale3 Abspack program implemented in CrysAlisPro. The structure was solved by the direct method and refined by the full matrix least-squares in the anisotropic approximation for all atoms using SHELXTL software⁷ implemented in the X-Seed program package.⁸ The X-ray diffraction experimental details and crystallographic characteristics of Co_5B_{16} are presented in Table 1 and Table 2. The DIAMOND software⁹ was used to create molecular graphics.

The crystallographic data of Co_5B_{16} and further details of the crystal structure investigation have been deposited in the Inorganic Crystal Structure Database¹⁰ and may be obtained free of charge from Fachinformationszentrum Karlsruhe, 76344 Eggenstein-Leopoldshafen, Germany (fax: (+49)7247-808-666; e-mail: crysdata@fiz-karlsruhe.de, http://www.fiz-karlsruhe.de/request_for_deposited_data.html) on quoting the deposition number CSD-427205.

2.3. Hardness measurements

Vickers hardness (H_v) was measured using a microhardness tester (M-400-G2, LECO Corporation) under loads of 0.5 kgf (4.9 N), 1 kgf (9.8 N) and 1.5 kgf (14.7 N). The average value of hardness was found to be $H_v = 30.1 \pm 2$ GPa.

2.4. Magnetic properties

Magnetic susceptibility was measured with the MPMS SQUID magnetometer in the temperature range 2–380 K in magnetic fields up to 5 T. Heat capacity measurements were attempted with Quantum Design PPMS in zero field using relaxation technique, but no detectable signal could be obtained because of the diminutively small sample size.

2.5. Electronic structure calculations

Electronic structure of Co_5B_{16} was calculated in the framework of density functional theory (DFT) using the FPLO code¹¹ and Perdew-Wang flavor of exchange-correlation potential (LDA).¹² Reciprocal space was sampled with 135 k -points in the symmetry-irreducible part of the first Brillouin zone, and the convergence with respect to the number of k -points has been carefully checked.

3. Results and discussion

3.1. Crystal structure of Co_5B_{16}

Single-crystals of Co_5B_{16} were synthesized at the pressure of 15 GPa and the temperature of 1873–1573 K. The structure of Co_5B_{16} is orthorhombic ($Pmma$ space group, Tables 1-4). Similar to structures of other boron-rich metal borides, it can be described based on a rigid network of boron atoms. In Co_5B_{16} one can easily see honeycomb-like stripes (Fig. 1) oriented along the b -axis and condensed into a complicated ramous structure. Such an arrangement of boron atoms gives rise to the straight, channel-like voids along the b -axis. Cobalt atoms occupy these voids creating infinite rows. Metal-metal distances in the rows are all equal, but they are

larger than the sum of metallic radii of Co atoms (see Table 4). This is similar to the arrangement of metal atoms in other B-rich transition-metal borides, such as CrB₄ and FeB₄,^{2,13} but different from that in MnB₄. Although MnB₄ has the structure closely related to that of CrB₄ and FeB₄, Mn–Mn distances in MnB₄ are not equal due to the Peierls distortion.^{14,15}

Despite some allusion to the tetraboride CrB₄ and FeB₄ structures, the Co polyhedra in Co₅B₁₆ are distinctly different. The Co atoms occupy three independent crystallographic sites, Co(1), Co(2) and Co(3) (Table 2). The structure of Co₅B₁₆ can be visualized in terms of packing of three kinds of Co-B polyhedra (Figure 1). An asymmetric part of the structure (Fig. 1a) consists of three units: an irregular Co(3)B₁₂ polyhedron, its distorted counterpart Co(1)B₁₂, and a Co(2)B₉ polyhedron. Polyhedra of each kind (Co(2)B₉, Co(1)B₁₂ and Co(3)B₁₂) pack in columns by sharing common upper and bottom faces and create their own infinite columns parallel to the *b*-axis (Fig. 1b). Co(1)B₁₂ polyhedra, as well as Co(3)B₁₂ ones, share the opposite parallelogram-shaped faces, which are parallel to the *ac*-plane. The Co atoms in these columns have the same *y*-coordinates. Co(2)B₉ polyhedra pack *via* common triangular faces and each polyhedron sticks to the neighboring Co(1)B₁₂ one through a side quadrilateral face (Fig. 1b). As a result Co(1)- and Co(2)- atoms in neighboring columns are shifted on *b*/2 along the *b*-axis. A polyhedron topologically similar to Co(2)B₉ can be deduced from the Co(3)B₁₂ one by removing at once vertices of the two parallelogram-shaped faces of CoB₁₂ and one vertex from the rectangular in the equatorial plain of the latter.

The Co-B distances in Co(3)B₁₂ vary from 2.015(5) to 2.304(4) Å and an average value is 2.183(5) Å (Table 3). Co(1)B₁₂ shares two of its side quadrilateral faces with the Co(2)B₉ polyhedra (see Fig. 1). This leads to a distortion of the Co(1)B₁₂ geometry compared to that of Co(3)B₁₂: the Co-B distances' range is 1.991(5) to 2.475(4) Å and an average value increases to 2.275(5) Å. Due to the smaller coordination number of Co(2), the Co(2)B₉ polyhedron is the most compact with the average <Co(2)–B> distance of 2.141(7) Å.

Figure 2 provides a comparison of the structure of Co₅B₁₆ with that of *MB*₄ tetraborides, where *M* = Cr, Fe, Mn.^{2,13,14} In tetraborides, there is only one kind of *MB*₁₂ polyhedra packed in columns (Fig. 2b), so that each column is shifted on *c*/2 along the *c*-axis with respect to its four nearest neighbors (shown in different colors, light and dark). In Co₅B₁₆, every column of Co(3)B₁₂ polyhedra has four neighboring Co(1)B₁₂ columns and shares common B(5) vertices

with two of them, while the other two are attached by common edges, which form ...–B(6)–B(9)–B(6)–... zigzag chains (Fig. 2a).

The B–B distances in the structure of Co_5B_{16} vary from 1.654(7) to 1.908(7) Å (Table 4). The shortest bond located at the *ac* plane is observed between B atoms of the neighboring Co(3)B12 and Co(1)B12 polyhedra. This is the smallest value of the B-B bond length among transition metal borides with related structures (Table 4). Dense atomic packing and short B-B contacts make Co_5B_{16} rather hard with the measured Vickers hardness $H_v = 30 \pm 2$ GPa, the value slightly higher than reported for CrB_4 ,¹³ but lower than that of superhard FeB_4 .²

3.2. *Magnetic and electronic properties of Co_5B_{16}*

Similar to FeB_4 , the preparation of single-phase samples of Co_5B_{16} is exceedingly difficult. The largest phase-pure sample available so far is about 0.4 mg and can be used for magnetization measurements only. Magnetic susceptibility shown in Fig. 3 exhibits a weak temperature dependence and a more pronounced field dependence that is likely related to trace amounts of a ferromagnetic impurity. In higher magnetic fields, the impurity signal is suppressed, and a residual temperature-independent susceptibility of about $\chi_0 = 2 \times 10^{-4}$ emu/mol is observed (Fig. 3). Therefore, Co_5B_{16} behaves as a standard Pauli paramagnet. Small humps in the susceptibility below 100 K require further investigation. Our measurements in low magnetic fields did not show any signatures of superconductivity above 2 K.

Electronic structure of Co_5B_{16} suggests metallic behavior (Fig. 4), with a relatively high density of states at the Fermi level: $N(E_F) \sim 1 \text{ eV}^{-1}/\text{Co}$, similar to $1 \text{ eV}^{-1}/\text{Fe}$ in FeB_4 .¹ By correcting our experimental χ_0 for the core diamagnetism $\chi_{\text{dia}} \sim -2 \times 10^{-4}$ emu/mol,¹⁶ we arrive at the Pauli contribution $\chi_{\text{Pauli}} = \chi_0 - \chi_{\text{dia}} \sim 4 \times 10^{-4}$ emu/mol that is comparable, yet larger than the value of 1.6×10^{-4} emu/mol expected from our calculated $N(E_F)$.

The states at the Fermi level are of mixed Co *3d* and B *2p* origin, but most of the Co *3d* states are below the Fermi level and form a relatively narrow band complex between -3 eV and the Fermi level (Fig. 4). These narrow bands should host more localized electrons that tend to become magnetic. In Co_5B_{16} , the complete filling of these localized states excludes the magnetism. Indeed, spin-polarized calculations for Co_5B_{16} always converge to the non-magnetic solution.

4. Conclusions

In conclusion, the novel boron-rich cobalt boride Co_5B_{16} synthesized at high-pressure and high-temperature conditions was found to be non-magnetic that is in line with the trend of the reduced magnetism upon the decrease in the TM:B ratio. Indeed, Co_3B ($T_C = 747 \text{ K}$)¹⁷ and Co_2B ($T_C = 433 \text{ K}$)³ are ferromagnetic, whereas CoB ³ and the Co_5B_{16} are non-magnetic metals. Early studies¹⁸ argued that the behavior of TM-rich borides resembles that of pure transition metals, because boron atoms simply change electron concentration in the TM $3d$ bands. Apparently, this no longer holds for B-rich TM borides, where a large contribution of boron states is present at the Fermi level (see Fig. 4), and Pauli-paramagnetic behavior is observed.

5. Acknowledgements

A.T. was supported by the Mobilitas grant MTT77 from the ESF. We thank Deepa Kasinathan and Valeriy Verchenko for technical assistance in magnetic susceptibility measurements. H.G. gratefully acknowledges financial support of the Alexander von Humboldt Foundation. The work was supported by the German Research Foundation (DFG). N.D. thanks the DFG for financial support through the Heisenberg Program and the DFG research grant (No. DU 954-8/1).

6. References

- ¹Kolmogorov, A.N.; Shah, S.; Margine, E.R.; Bialon, A.F.; Hammerschmidt, T.; Drautz, R. *Phys. Rev. Lett.* **105**, 217003 (2010).
- ²Gou, H.; Dubrovinskaia, N.; Bykova, E. *et al.* *Phys. Rev. Lett.* **111**, 157002 (2013).
- ³Cadeville, M.-C.; Meyer, A.J.-P. *C. R. Acad. Sci. (France)* **255**, 3391(1962).
- ⁴Isnard, O.; Fruchart D. *J. Alloys Comp.* **205**, 1(1994).
- ⁵Ito, E., in *Treatise on Geophysics*, edited by G.D. Price (Elsevier, Amsterdam, 2007), Vol. 2, pp. 198–230.
- ⁶Agilent Technologies, Agilent Technologies UK Ltd., Oxford, UK, Xcalibur CCD system, CrysAlisPro Software system, Version 1.171.35.19 (2012).
- ⁷Sheldrick, G.M. *Acta Crystallogr. Sect. A Found. Crystallogr.* **64**, 112 (2008).
- ⁸Barbour, L.J. *J. Supramol. Chem.* **1**, 189 (2001).
- ⁹Brandenburg, K. DIAMOND, Crystal Impact GbR, Bonn, Germany (1999).

- ¹⁰Belsky, A.; Hellenbrandt, M.; Karen, V. L. *et al.* [Acta Crystallogr. B](#) **58**, 364 (2002).
- ¹¹ Koepernik, K.; Eschrig, H. [Phys. Rev. B](#) **59**, 1743 (1999).
- ¹² Perdew, J.P.; Wang, Y. [Phys. Rev. B](#) **45**, 13244 (1992).
- ¹³Knappschneider, A.; Litterscheid, C.; Dzivenko D. *et al.* [Inorg. Chem.](#) **52**, 540 (2013).
- ¹⁴Gou H., Tsirlin A.A., Bykova E. *et al.*, [Phys. Rev. B](#) **89**, 064108 (2014).
- ¹⁵Knappschneider, A.; Litterscheid, C.; George, N.C.; Brgoch, J.; Wagner, N.; Beck, J.; Kurzman, J.A.; Seshadri, R.; Albert B. [Angew. Chem. Int. Ed.](#) **53**, 1684 (2014).
- ¹⁶König, E.; König, G. Magnetic Properties of Coordination and Organometallic Transition Metal Compounds, published in *Landolt-Börnstein - Group II Molecules and Radicals* (1981) *II*, 1.
- ¹⁷Fruchart, R. [C. R. Acad. Sci.](#) **256**, 3304 (1963).
- ¹⁸Lundquist, N., Myers, H.P., Westin, R. [Phil. Mag.](#) **7**, 1187 (1962).

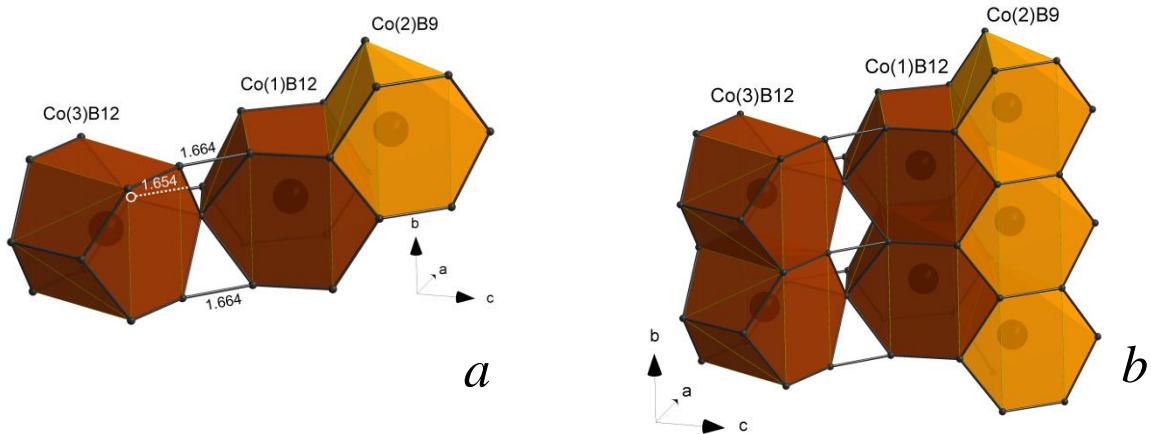


FIG. 1. A polyhedral model of the structure of Co_5B_{16} . (a) An asymmetric part of the structure consisting of three units: an irregular Co(3)B12 polyhedron, its distorted counterpart Co(1)B12, and a Co(2)B9 polyhedron. (b) Packing of the polyhedra in columns along the b -axis by sharing common faces. The y coordinates of Co atoms in light and dark polyhedra differ by $1/2$. B–B bonds are highlighted by bold lines, the shortest distances are labeled.

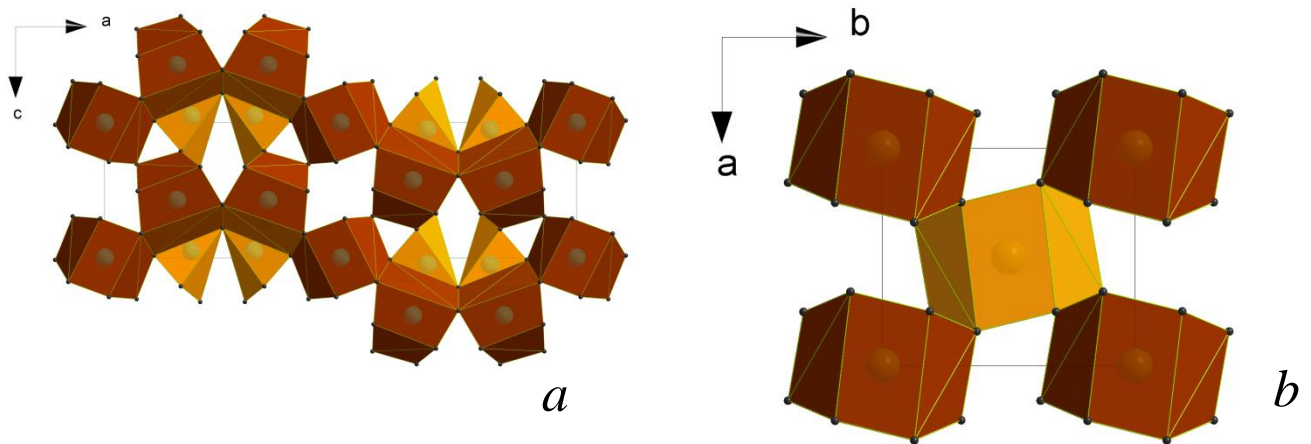


FIG. 2. Comparison of the crystal structures of Co_5B_{16} and MB_4 ($M = \text{Cr}, \text{Fe}, \text{Mn}$)^{5,2,6}. (a) Co_5B_{16} ; (b) MB_4 . In the both structures MB12 polyhedra pack in columns by sharing common parallelogram-shaped faces either along the b - (Co_5B_{16}) or c -axis (MB_4). Co_5B_{16} contains columns constructed of Co(2)B9 polyhedra. Light and dark polyhedra differ in position along b - or c -axis, respectively.

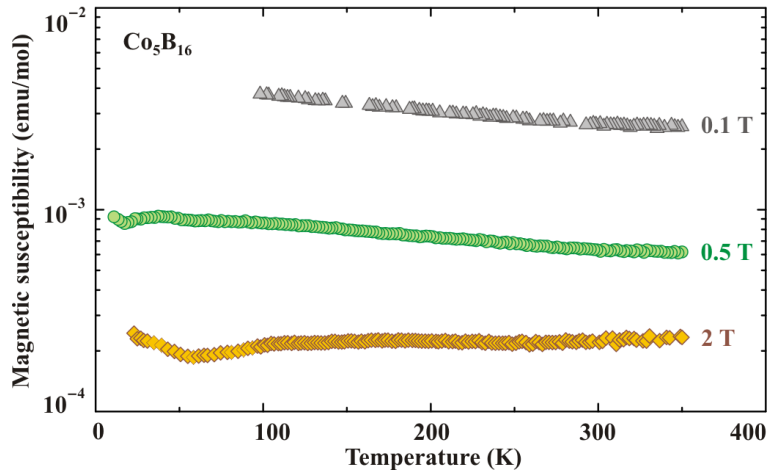


FIG. 3. Magnetic susceptibility of Co_5B_{16} measured in the applied fields of 0.1 T, 0.5 T, and 2 T. In the 0.1 T data, some of the data points were removed because of the low signal and strong noise.

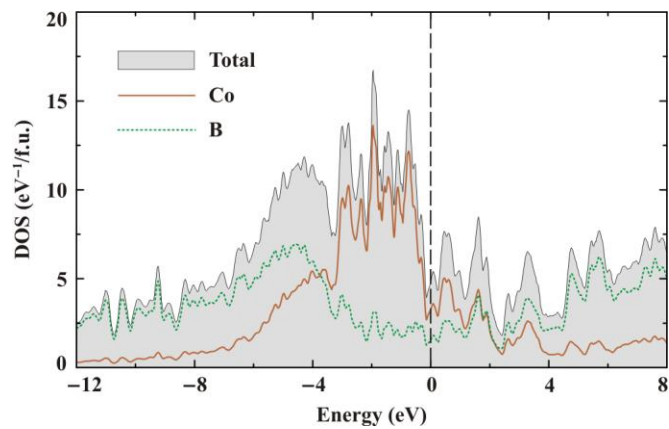


FIG. 4. LDA density of states (DOS) for Co_5B_{16} . The total DOS is shown by shading. The solid and dotted lines denote the Co and B contributions, respectively. The Fermi level is at zero energy.

Table 1. Experimental details and crystallographic characteristics for Co₅B₁₆

Empirical formula	Co ₅ B ₁₆
Formula weight (g/mol)	467.61
Temperature (K)	296(2)
Wavelength (Å)	0.7107
Crystal system	Orthorhombic
Space group	<i>Pmma</i>
<i>a</i> (Å)	19.1736(12)
<i>b</i> (Å)	2.93290(10)
<i>c</i> (Å)	5.4886(2)
<i>V</i> (Å ³)	308.65(2)
<i>Z</i>	2
Calculated density (g/cm ³)	5.032
Linear absorption coefficient (mm ⁻¹)	13.061
F(000)	430
Crystal size (mm ³)	0.07 x 0.05 x 0.05
Theta range for data collection (deg.)	3.71 to 30.48
Completeness to theta = 25.00°	99.7 %
Index ranges	-20 < <i>h</i> < 27, -4 < <i>k</i> < 4, -7 < <i>l</i> < 7
Reflections collected	3345
Independent reflections / <i>R</i> _{int}	569 / 0.0532
Max. and min. transmission	0.5612 and 0.4617
Refinement method	Full matrix least squares on <i>F</i> ²
Data / restraints / parameters	569 / 0 / 67
Goodness of fit on <i>F</i> ²	1.145
Final <i>R</i> indices [<i>I</i> > 2σ(<i>I</i>)]	<i>R</i> ₁ = 0.0282, <i>wR</i> ₂ = 0.0544
<i>R</i> indices (all data)	<i>R</i> ₁ = 0.0370, <i>wR</i> ₂ = 0.0569
Largest diff. peak and hole (e / Å ³)	0.869 and -0.882

Table 2. Atomic coordinates, positions and equivalent isotropic displacement parameters for Co₅B₁₆.

Atom	Wykoff site	<i>x</i>	<i>y</i>	<i>z</i>	$U_{\text{eq}}^a, \text{\AA}^2$
Co(1)	4 <i>i</i>	0.15330(3)	0	0.57345(11)	0.0048(2)
Co(2)	4 <i>j</i>	0.18369(3)	0.5	0.95008(12)	0.0046(2)
Co(3)	2 <i>a</i>	0	0	0	0.0045(2)
B(1)	2 <i>e</i>	0.25	0	0.7796(14)	0.0067(14)
B(2)	4 <i>i</i>	0.1614(3)	0	0.2119(9)	0.0044(9)
B(3)	4 <i>j</i>	0.0700(3)	0.5	0.5066(10)	0.0062(9)
B(4)	2 <i>f</i>	0.25	0.5	0.6068(14)	0.0073(14)
B(5)	4 <i>i</i>	0.678(3)	0	0.3065(10)	0.0061(10)
B(6)	4 <i>i</i>	0.1050(2)	0	0.9840(10)	0.0048(9)
B(7)	4 <i>j</i>	0.2026(3)	0.5	0.3273(10)	0.0055(9)
B(8)	4 <i>j</i>	0.0091(3)	0.5	0.2906(9)	0.0064(10)
B(9)	4 <i>j</i>	0.0772(3)	0.5	0.8208(10)	0.0056(10)

^a U_{eq} is defined as one third of the trace of the orthogonalized U^{ij} tensor.

Table 3. Co...B interatomic distances in CoB12 and CoB9 polyhedra (in Å)

Co(1)B12			Co(2)B9			Co(3)B12		
Co(1)–B(2)	1x	1.991(5)	Co(2)–B(2)	2x	2.097(4)	Co(3)–B(2)	2x	2.015(5)
Co(1)–B(1)	1x	2.172(4)	Co(2)–B(7)	1x	2.102(5)	Co(3)–B(7)	2x	2.126(5)
Co(1)–B(5)	1x	2.198(5)	Co(2)–B(6)	2x	2.112(3)	Co(3)–B(6)	4x	2.174(4)
Co(1)–B(3)	2x	2.199(4)	Co(2)–B(1)	2x	2.155(3)	Co(3)–B(1)	4x	2.304(4)
Co(1)–B(7)	2x	2.206(4)	Co(2)–B(9)	1x	2.162(5)			
Co(1)–B(4)	2x	2.3709(8)	Co(2)–B(4)	1x	2.273(7)			
Co(1)–B(6)	1x	2.436(5)						
Co(1)–B(9)	2x	2.475(4)						
<Co(1)–B>		2.275(5)	<Co(2)–B>		2.141(7)	<Co(3)–B>		2.183(5)

Table 4. Interatomic distances in metal borides with related structures.

Metal boride	$M-M$ distances, Å	$M-B$ distances, Å	$B-B$ distances, Å	Reference
Co_5B_{16}	2.9329(1)	1.991(5)–2.475(4)	1.654(7)–1.908(7)	This work
CrB_4	2.8681(5)	2.053(4) 2.153(4) 2.178(3) 2.261(3)	1.743(6) 1.835(4) 1.868(6)	[13]
FeB_4	2.9990(3)	2.009(4) 2.109(4) 2.136(3) 2.266(3)	1.714(6) 1.8443(3) 1.894(6)	[2]
MnB_4	2.7006(6), 3.1953(7)	1.999(4)–2.310(4)	1.703(6)–1.893(8)	[14]